ASEAN Engineering Journal

Full Paper

CFD SIMULATION OF A TRANSIENT ULTRAFILTRATION SYSTEM FOR CONCENTRATING BROMELAIN FROM PINEAPPLE WASTES

Le Tan Duc[a,b], Duong Hoang Phi Yen[a,b], Le Minh Tan[a,b], Hoang Long[a,b], Tran Tan Viet[a,b*]

[a]Faculty of Chemical Engineering, Ho Chi Minh City University of Technology (HCMUT), 268 Ly Thuong Kiet Street, Ho Chi Minh City, Vietnam
[b]Vietnam National University Ho Chi Minh City (VNU-HCM), Linh Trung ward, Thu Duc District, Ho Chi Minh City, Viet Nam

Article history
Received
20 August 2023
Received in revised form
22 December 2023
Accepted
11 February 2024
Published online
31 August 2024

*Corresponding author
trantanviet@hcmut.edu.vn

Graphical abstract

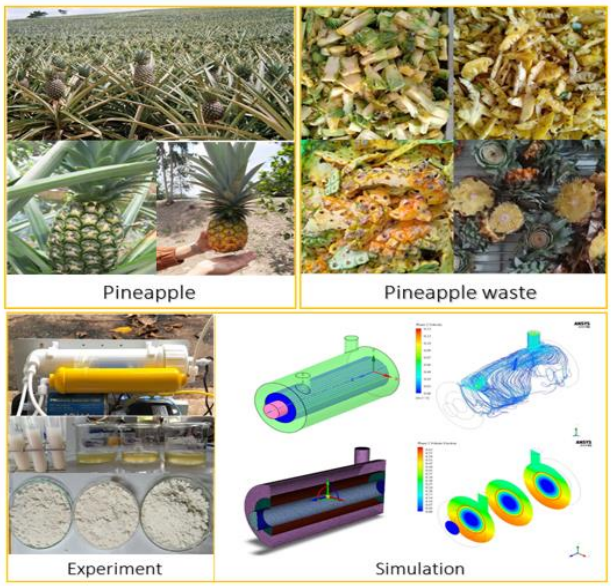

Abstract

In this research, using an ultrafiltration (UF) membrane to purify bromelain enzyme during the production of bromelain enzyme from pineapple brings high efficiency in product quality. This study evaluated membrane filtration using computational fluid dynamics (CFD) simulations. First, the simulation builds a computational model based on the actual UF module to evaluate the filtration performance and the fluid behavior through the filter. Additionally, The Navier – Stokes equations and conservation equations are used to solve the conditions in the study of membrane filtration. The transient mode is used, corresponding to a time level of 3500s. Under the turbulent flow model (SST k–ω), it is necessary to predict the velocity and pressure behavior as well as the parameters of the fluid inside the equipment. The results show that the bromelain enzyme obtained is 99.17%, and the maximum pressure when the process is stable is 236 kPa. The simulation shows that the mathematical model and the simulation results are consistent with validated experimental data.

Keywords: bromelain, CFD, ultrafiltration, simulation, modeling.

1.0 INTRODUCTION

Vietnam is a country in Southeast Asia with great potential for horticulture because of its tropical climate, which is favorable for many kinds of fruit. Pineapple (*Ananas comosus L.*) is a fruit that is grown a lot, spreading from the north to the south of Vietnam [1,2]. Pineapple is a source rich in vitamins and minerals [3], for example, a ripe pineapple can provide about 16% vitamin C daily [4]. However, in the fruit processing industry, pineapple produces about 45-55% of waste [5]. Besides, pineapple waste can arise from pineapple farms such as leaves, stems, roots, and damage to the pineapple after harvest. The pineapple tree is estimated to be more than 6 kg of fresh waste if 12,000 trees are planted on an acre of land, generating more than 70 tons of solid waste [6]. Therefore, it is necessary to have appropriate treatment methods to prevent environmental pollution and utilize them for processing into other valuable materials or applications.

The recent emphasis on extracting the enzyme bromelain from pineapples is crucial due to its special applications in industries such as food, cosmetics, and pharmaceuticals. For example, the present study indicates that bromelain combined with donepezil has the ability to neuroprotection, and limit cognitive impairment, which promises to be a study that makes a great contribution to the treatment of Alzheimer's disease [7]. Moreover, bromelain produced from pineapple waste is a great

advantage in terms of cost than using the fruit [8–11]. The circular economy of solid waste from pineapples contributes to the green economy by reducing deforestation and direct carbon dioxide emissions and increasing the revenue for processing facilities in Vietnam. As a result, the extraction of bromelain from pineapple by-products can develop the sustainable use of high-value products from the waste pineapple, which even so, is a good way towards economic development and environmental friendliness [11].

In addition to studies on the extraction of bromelain enzyme, extensive research on the purification of bromelain from pineapple has attracted appreciable attention, especially the application of membrane technology. Membrane technology is one of the most significant solutions for water treatment as well as protein separation fields which requires high-quality products, and green technology due to the lack of chemical requirements [12,13][13-16]. The application of membrane technology in the separation of bromelain has been studied extensively. Lopes et al. [16] set up an experimental two-stage membrane process to investigate the influence of pH and transmembrane pressure by using a plane microfiltration membrane at the first step. After that, the enzyme continues to purification by a 10 kDa ultrafiltration membrane at the second step with 90% bromelain recovery. According to Nor et al. [17], an ultrafiltration process combined with 2 stages with 75 kDa and 10 kDa tubular ceramic membranes has been successfully proposed for bromelain purification. The instrument was operated at v = 7.5 m/s^{-1} and pH = 4.0 conditions. The research results show that the membrane filtration process is successfully applied, ensuring the activity of the enzyme bromelain. Doko et al. (1991) investigated the use of sequential batch filtration, consisting of microfiltration (8µm) and ultrafiltration (100 kDa), before lyophilization of the residue during filtration to be removed through a binding method. ammonium precipitation and ultracentrifugation, the recovery yield was 50% [18]. However, there are still some active problems, especially the efficiency of the separation process, and membrane clogging owing to the physical properties of the inlet stream as well as the filter flux. Recent advances in protein separation, such as membrane filtration, can be applied to successfully utilize this technology in bromelain purification. However, conventional membrane separation methods continue to have flux and entrance stream characteristics, particularly viscosity, challenges. Furthermore, process modification is required to enhance extraction efficiency, minimize oxidation, prevent denaturation, and promote protein absorption. Assessment on a larger scale necessitates high precision as well as significant implementation costs and takes a long time. To break through this barrier, numerical approaches like CFD (computing fluid dynamics) simulations are a good way to validate experimental models and compare results. The application of CFD on membrane technology has been conducted recently. In 2020, a study simulated whey protein ultrafiltration, showing protein concentration polarization over time increased membrane resistance and reduced permeate flux. Haribabu et al [19] demonstrated the importance of accounting for concentration polarization in predictive modeling of protein ultrafiltration processes. According to Marcos [20], a computational fluid dynamics (CFD) model was presented to simulate momentum and concentration equations during ultrafiltration using the finite element method. The CFD model couples the Navier-Stokes equations with a resistance model linking protein concentration, feed velocity, permeate flux, and membrane surface pressure to predict transient permeate flux and pressure compared well to experimental soy protein concentrate concentration data. Based on our current understanding, there has been no prior research on the application of Computational Fluid Dynamics (CFD) for the ultrafiltration membrane in purifying bromelain enzyme.

To the best of our knowledge, the efficiency of the filtration process is highly dependent on the geometrical structure and the operating conditions of the membrane. Parameter values in both axial and radial directions, which can be formed by the nature of the fluid and the structure of the membrane, affect the filtration efficiency and the post-filtration concentration [21]. In this study, the use of CFD simulation aims to evaluate the behavior of the fluid inside the filtration module, thereby verifying the simulation results by comparing it with the experimental filtration of bromelain enzyme (extracted from pineapple by-products). The study revealed the internal flow distribution, understanding of the design, and improving the effective filtration method in the future.

2.0 METHODOLOGY

2.1 Development of The Model

The ceramic membrane filter, primarily made of titania, is a tube-shell equipment with the geometry principle illustrated in Figure 1. The equipment consists of a cylindrical shell and a tubular filter inside. The inlet is tubular with a circular cross-section through which the fluid flows into the module tangentially to the filter, the outlet is also tubular and is designed for a concentrated stream outlet. When the fluid enters, the smaller components will permeate through the porous medium of the filter membrane into the permeable flow, whereas the larger components will be retained and collected at the concentrator end.

The feed inlet in this model is assumed to only have 2 components, water and bromelain enzyme. The impurities in the feedstock is assume to be ignored.

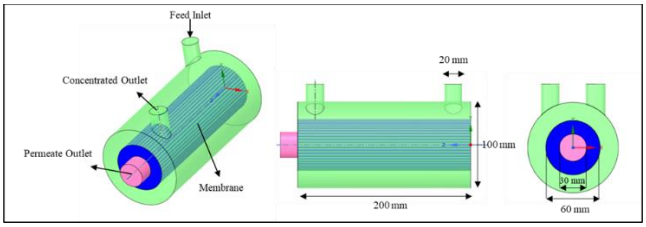

Figure 1 The geometry and dimensions of the ceramic membrane

A 3D mesh was built by using a polyhedra grid with 450,937 cells and 1,748,247 nodes as shown in Figure 2. The quality of the grid is acceptable in that the skewness and orthogonality average qualities are 0.19 and 0.85, respectively.

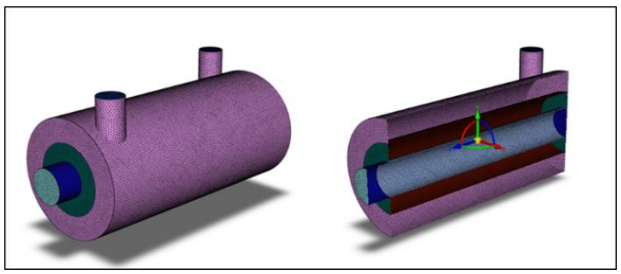

Figure 2 The polyhedra grid of the membrane module

2.2 Numerical Methods

A three-dimensional (3D) CFD of the ceramic membrane module to explore the hydrodynamics and performance of the bromelain ultrafiltration (UF). ANSYS Fluent software was used to solve the model equations in the feedstock, concentrated, and permeate streams with the proposed boundary conditions. The finite volume method (FVM) for the numeric dissolving of the equations is applied [22]. In this investigation, the inlet flow into the membrane module is a combination of bromelain and water. It is observed that the bromelain enzyme is soluble in water[23]. In order to describe the multiphase flow inside the module, the Eulerian model and the Shear-Stress Transport (SST k–ω) model were utilized as described by Neto et al [24]. In the multiphase model, we introduce the volume fraction (α_p) for the calculated phase (denoted by subscript "p"). This inclusion aims to examine how each phase occupies volume in relation to the total cell volume. Within each cell, the laws of mass and linear momentum conservation are maintained separately for each phase. Therefore, the control volume of each phase is given by:

$$V_q = \int_V \alpha_p dV$$

where: $\sum_{q=1}^{n} \alpha_p = 1$

The feed inlet in this model assumes only two components: water and the bromelain enzyme. Impurities in the feedstock are disregarded. Consequently, a multiphase approach is applied, wherein the bromelain, representing the granular phase, is well dispersed in water, the continuous phase. The equations of the moment and continuity are assumed to be solved for the same pressure, as are the conditions of conservation of mass and linear moment for each phase [25,26].

The mass conservation equation is given by:

$$\frac{\partial}{\partial t}(\alpha_q \rho_q) + \nabla \cdot (\alpha_q \rho_q \vec{v}_q) = 0$$

where "q" represents the water or bromelain phase in the mixture; α is the volumetric fraction; ρ and $\vec{v}$ are the density, and velocity vectors, respectively.

Equation of momentum defined by:

$$\nabla \cdot (\alpha_q \rho_q \vec{v}_q \vec{v}_q) = -\alpha_q \nabla \mathrm{P} + \nabla \cdot \bar{\tau}_q + \alpha_q \rho_q \vec{g} + \sum_{\mathrm{p=1}}^{\mathrm{n}} \vec{\mathrm{R}}_{\mathrm{pq}}$$

where $\vec{R}_{pq}$, $\bar{\bar{\tau}}_q$ and P is an interaction force between phases, the stress tensor, and the pressure shared by all phases, respectively.

The stress tensor is defined by:

$$\bar{\bar{\tau}}_{\mathrm{q}} = \alpha_{\mathrm{q}} \mu_{\mathrm{q}} \left(\nabla \vec{\mathrm{v}}_{\mathrm{q}} + \nabla \vec{\mathrm{v}}_{\mathrm{q}}^{T}\right) + \alpha_{\mathrm{q}} \left(\lambda_{\mathrm{q}} - \frac{2}{3}\mu_{\mathrm{q}}\right) \nabla \cdot \vec{\mathrm{v}}_{\mathrm{q}} \bar{\bar{\mathrm{I}}}$$

Here μ_q and λ_q are the shear and bulk viscosity of phase q, and $\bar{\bar{I}}$ is the unit tensor.

The interaction force between water and bromelain phases $\vec{R}_{pq}$ defined by:

$$\sum_{p=1}^{n} \vec{R}_{pq} = \sum_{p=1}^{n} K_{pq}(\vec{v}_p - \vec{v}_q),$$

Here $\mathrm{K_{pq}}$ is the interfacial momentum transfer coefficient; v is the velocities of the phase.

The interfacial momentum transfer coefficient is defined by:

$$\mathrm{K_{pq}} = \frac{\rho_{\mathrm{p}} \mathrm{f}}{6\tau_{\mathrm{p}}} \mathrm{d_p A_i}$$

where f, A_i are the drag function and the interfacial area, respectively.

The term τ_p is the "particulate relaxation time", defined as follows:

$$\tau_p = \frac{\rho_p d_p^2}{18\mu_q}$$

where d_p is the diameter of the drop.

The Schiller and Naumann model [27] was used to describe the drag function f in interfacial momentum transfer, as follows:

$$\mathrm{f} = \frac{\mathrm{C_D} Re}{24}$$

Here C_D, is the drag coefficient, Re is the relative Reynolds.

In the porous region, the multi-phase model and governing equations for mass and linear momentum are applied similarly to the non-porous zone. However, in ANSYS Fluent software, the porous zone is modeled as a fluid element zone. The modification of the linear momentum occurs through a change in the source term, which comprises two parts: the loss of viscosity, represented by Darcy's Law, and the loss of inertia. In this research, the porous zone is homogeneous, and therefore, the source term is given by:

$$\mathrm{S_i} = -\left(\frac{\mu}{K_i} \mathrm{v_i} + \mathrm{C_2} \frac{1}{2} \rho |\mathrm{v}| \mathrm{v_i}\right)$$

where i-th is represented for the dimensional space (x, y, z) of the linear momentum equation, |v| is the magnitude of the velocity, K_i is the permeability and C_2 is the inertial resistance factor.

The boundary conditions used for the simulation of bromelain enzyme filtration by membrane filtration are presented in Table 1. In which some parameters of input, output, and property parameters of each strain are presented at operating conditions of 101325 Pa following the experimental setup. Additionally, the material properties used in this simulation are described in Table 2, and the permeability (K) is 4.18 x 10^{-18} m^2 and the membrane porosity is 60 % were chosen.

Table 1 Boundary conditions

	Parameters
Inlet	Mass flow inlet Bromelain: 0.005 kg/s Volume fraction: 0.1 Water: 0.01 kg/s
Concentrate outlet	Pressure outlet with a zero-gauge pressure outlet
Permeate outlet	Pressure outlet with a zero-gauge pressure outlet
Wall	Non-slip wall, null roughness, zero speed
Operation condition	101325 Pa

The Coupled algorithm was chosen to solve the continuous equation by the concatenation method with the goal of creating a lower convergence range than other separable solving algorithms [28,29]. The spatial customization for all original transport equations is in the first-order reverse direction while the pressure diagram uses PRESTO.

The physical properties of the materials used in this simulation are described in Table 2.

Table 2 Thermo-Physical Properties of Fluids and Material

Properties	Bromelain	Water	Titania
Density (kg/m^3)	1400	998.2	4230 [28]
Cp (j/kg.k)	3970 [29]	4182	683 [28]
Thermal Conductivity (w/m.k)	0.537 [30]	0.6	4.8 [28]
Viscosity (kg/m.s)	0.0015	0.001003	
Molecular weight (kg/kmol)	28000 [31]	18.0152	

2.3 Experimental Setup

To validate the simulation results, in this study, bromelain was isolated from pineapple wastes, including crown (40%), peel (40%), and fruit residues (20%). Firstly, pineapple wastes were cut into small pieces and extracted with phosphate buffer (pH 7.0) with the solid-liquid ratio (w/v) of 1:2 (g: mL) at room temperature for 10 mins. Afterward, the mixture was filtered through 35 microns filter cloth and then centrifuged at 3000 rpm for 25 minutes to remove any insoluble materials. The obtained liquid was continuously gone through a microfiltration system including a 1-micron water filter (poly-propylene), and a 0.2-micron filter (Polysulfone). For isolation and purification of bromelain, an ultrafiltration membrane system was developed including a 100kDa and 20kDa ceramic membrane. In the first stage, the feed from the microfiltration system was subjected to a cross-flow of UF membrane with a pore size of 100kDa. The high molecular weight molecules, such as polysaccharides, in the retentate flow, were separated from the low molecular weight bromelain (28kDa) in the permeate flow. The permeate continuously went through the 20kDa ceramic ultra-filter to obtain a bromelain solution in retentate flow. The quantity of bromelain was determined by the high-performance liquid chromatography (HPLC) method of Campos et al. [32]. The temperature change of the whole process was maintained at less than 10%. The mass flow of bromelain in this step was defined as the total weight of bromelain flow per total time of ultrafiltration.

3.0 RESULTS AND DISCUSSION

3.1 Distribution Of Water Volume Fraction

Figure 3 shows the distribution of water volume fraction inside the module at different times: 10s, 60s, 180s, 3500s. The volume fraction of water tends to decrease with time and has a low value in the lower region of the module. In addition, the volume ratio of water always reaches a maximum value of approximately 1 at the permeate flow, which means that the amount of bromelain hardly passes through the membrane to enter the permeable stream, indicating the membrane works with good efficiency and has high selectivity when most of the fluid passing through is water and remains very stable during the filtration process. Furthermore, as the filtration process takes longer, a ring forms around the membrane surface where the volume fraction of water is reduced to the lowest value due to the flow of water through the membrane. This indicates the formation of a bromelain layer on the membrane.

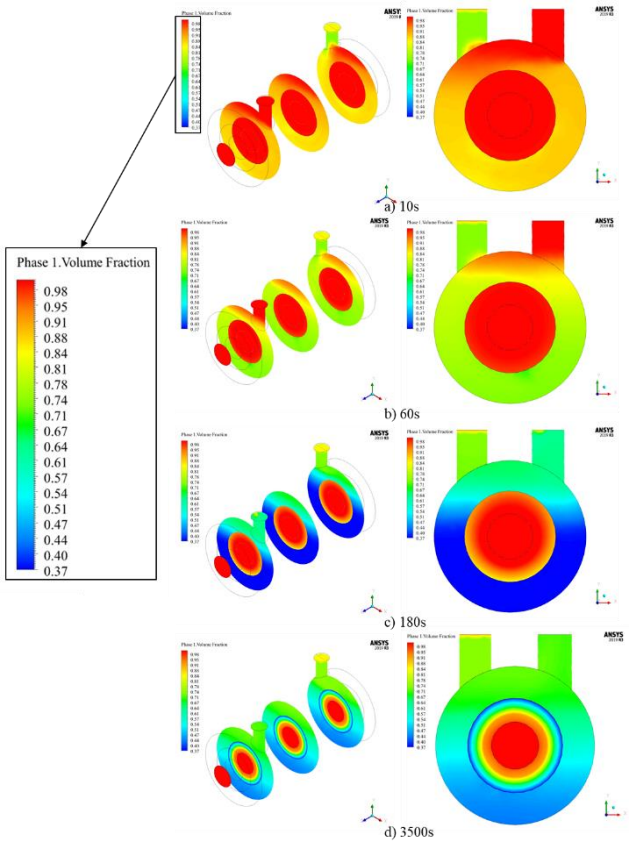

Figure 3 Distribution of water volume fraction at different times

In Figures 3a) and 3b), from 10s to 60s, when filtration takes place, as water is continuously filtered through the membrane entering the permeable stream and retaining the amount of bromelain inside the module, so the volume fraction of water will decrease. This value drops from 0.88 at 10s to 0.74 at 60s in most regions of the module. The longer the filtration time, the more bromelain concentrate in the module, thereby reducing the volume ratio of the water in the filter. This result can be observed in Figure 3c at 180s. At this time point, the water volume fraction reached the lowest value of 0.371.As can be seen from Figure 3, around the membrane surface exists an area with a water volume ratio of about 0.9 lower than other regions while at 10s and 60s this ratio is always maintained uniformly at 0.99 in the membrane. This means that bromelain has already begun to exist in the membrane, which can cause fouling and concentration polarization that interferes with filtration. This is shown more clearly in Figure 3d, at 3500s, the volume fraction

of water increases gradually with the thickness of the membrane and has the lowest value of 0.37 in the membrane area on the outer pipe side. At this time, water almost cannot pass through the membrane because the amount of bromelain has occupied the space in the membrane, hindering the separation process. Therefore, the inlet stream will mix with the amount of bromelain in the module causing an increase in the volume of water in the whole module. As can be seen from Figures 3c and 3d, this value increases from 0.37 to about 0.47 in the lower region of the module.

3.2 Distribution of Bromelain Volume Fraction

Regarding bromelain's volume fraction, this value's distribution will have the opposite behavior compared to that of water. This means that the volume fraction of bromelain in the module will increase over time as the amount of water is continuously filtered, shown in Figure 4. This value increases from about 0.12 at 10s to 0.26 at 60s. and reached a maximum value of 0.61 in most areas of the module. In addition, the volume fraction of bromelain at the concentrate outlet increased from 0 at 10s and 60s, to a maximum value of about 0.4 at 180s and then to 0.34 at 3500s. This is because at the beginning of filtration, as the water is passed through the permeate flow, bromelain will accumulate in the module but not enough to be able to come out of the concentrate outlet.

Until the 180s, bromelain has taken up most of the volume in the module, then mixes with the added inlet mixture and goes out at the concentrate outlet. At time 3500s from Figure 4d, when the water barely passes through the membrane into the permeate flow, the water will stay in the module and reduce the volume fraction of bromelain. The maximum value decreases from 0.61 to about 0.54. Furthermore, the volume fraction of bromelain at the membrane surface will increase with time until it occupies most of the membrane and interferes with filtration.

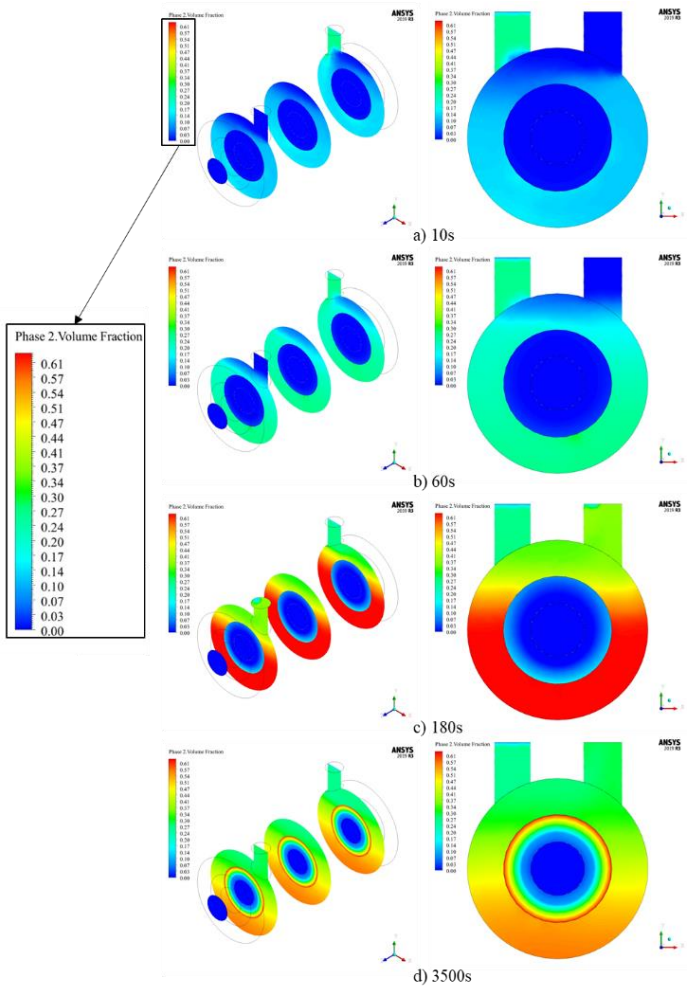

Figure 4 Distribution of bromelain volume fraction at different times

3.3 Distribution Of Streamline

Figure 5 shows the water flow at different times of 10s, 60s, 180s and 3500s, respectively. It can be observed that, from the beginning of the process to before 180s, water always passes through the membrane in a permeable stream. But the permeation flux decreases over time because bromelain accumulation at the membrane surface causes pore blocking or concentration polarization, until 3500s most water does not pass through the membrane into the permeable stream. At 180s, when the volume of water added is greater than the amount of water filtered out, the water starts to come out at the condensed outlet as shown in figure 5c.

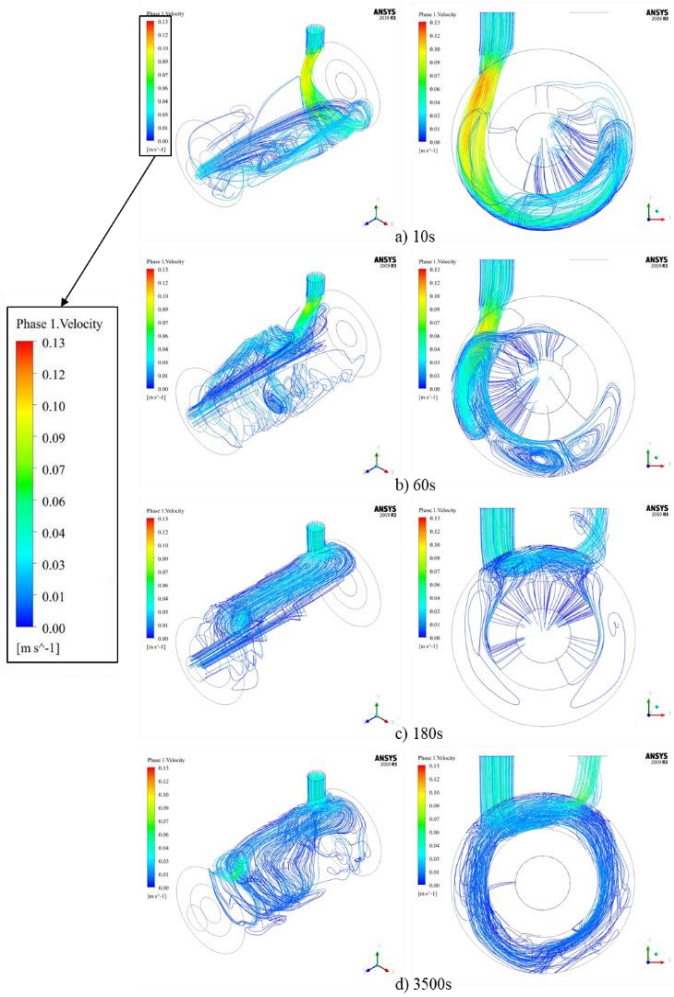

Figure 5 Streamline of water at different times

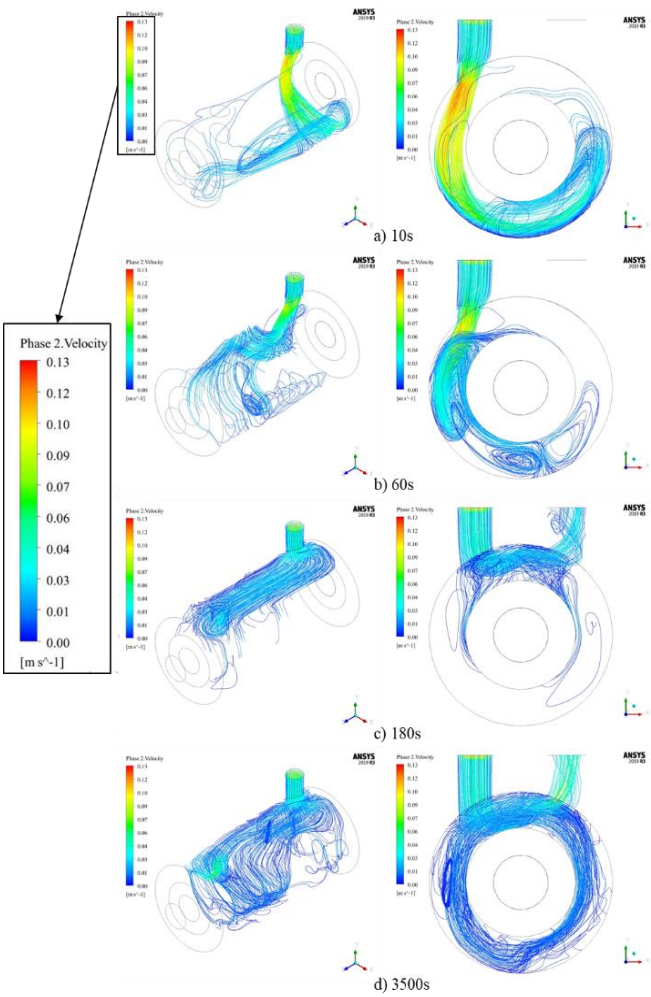

Figure 6 Streamline of bromelain at different times

It can be observed from Figure 6 that behavior of bromelain streamline is opposite to water, during the filtration process, the membrane blocks most of the bromelain and keeps it from going into the permeate flow. As the water phase passes through the membrane, the amount of bromelain retained in the bottom of the module increases until it takes up most of the volume in module and goes out at concentrate outlet from 180s to 3500s It can be seen that bromelain flow tends to go around on the membrane surface, causing fouling and concentration polarization.

3.4 Distribution Of Velocity

The results of the velocity distribution of water are shown in Figure 7 at the time points of 10s, 60s, 180s and 3500s. Observe at 10s and 60s, because most of the water pass through the membrane into permeate flow and leaves empty space in the module, so the water entering will have a large velocity in the inlet area and lower region of the module. At this time, the speed reaches the maximum value during the process is about 0.13 m/s^{-1} and then decreases as it goes away from this region. When the filtration is stable, from 180s to 3500s, the velocities at the inlet and outlet are maintained at a constant range from 0.04 to 0.05 m/s^{-1}.

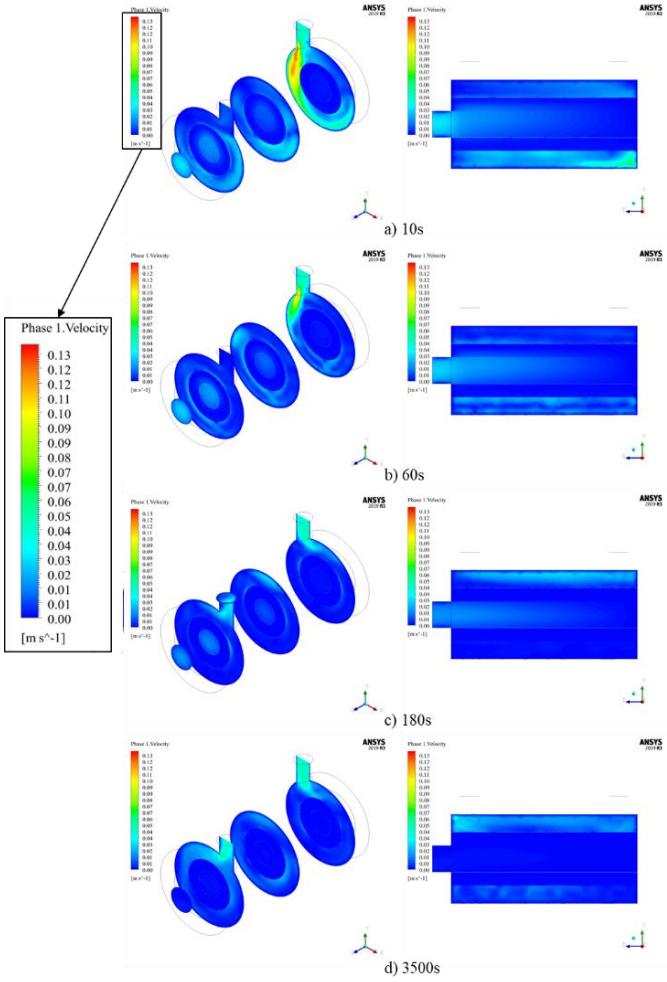

Figure 7 Distribution of water velocity

It can be seen that the velocity of water is higher in the inlet-outlet regions and the flow direction of the fluid. At the concentrate outlet, the velocity increases from 0 to about 0.39 m/s^{-1} over time and maintains this velocity from 180s to 3500s. Because the tangent flow of the input fluid enters the free space inside the equipment parallel to the membrane surface in a vortex shape, the area surrounding the membrane surface has a higher velocity than other parts. The velocity of the liquid flowing parallel to the membrane increases as a result. The results are compatible with Marcos et al. [25], which involved modeling the flow and temperature of the spiral membrane module.

At the beginning of the process, when the effect of hindering the filtration process is not significant, the water velocity inside the infiltration stream increases gradually from the inlet to the outlet region of the permeate. This happens during filtration because along the z-axis of the membrane the water is continuously filtered, through the membrane and into the permeate flow thus increasing the water flow velocity. This can be observed in Figure 7 at 10s and 60s. But from 180s to 3500s this speed-increasing area narrows because water is obstructed through the membrane by bromelain clinging to the membrane surface. Until 3500s, at this time, water almost does not pass through the membrane due to fouling or concentration polarization of bromelain, so the amount of water in the permeate flow is low and the velocity is almost zero.

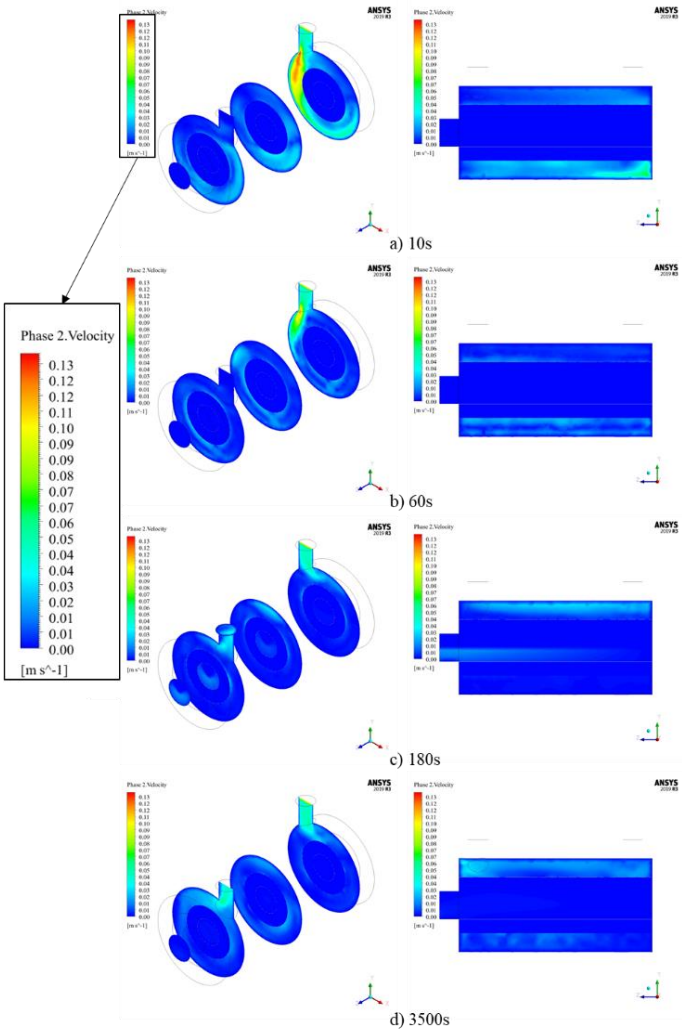

Figure 8 Distribution of bromelain velocity in the module

Figure 8 shows the velocity distribution of bromelain inside the module. The behavior of this distribution is similar to the velocity distribution of water. The regions near the inlet and the concentrate outlet have higher velocities than the rest, the velocities around the membrane surface tend to be greater than in the other regions. The difference is that the velocity of bromelain in the permeate is zero most of the time. But at time 180s, there appears a region with velocities from 0.1 m/s^{-1} to 0.2 m/s^{-1}. This happens because a small part of the bromelain will be carried by the water through the membrane slowly and when it enters the permeate, bromelain will follow the water and exit the permeate outlet.

3.5 Distribution Of Pressure

Figure 9 shows the module's pressure distribution at the xy and yz sections. It can be seen that along the z-axis at all times, the pressure is almost constant, and the area under the module has higher pressure than in other areas. The pressure in the module increased with time and kept stable for a long time at the inlet-outlet during the filtration process. In addition, the pressure at

the filter membrane decreases gradually in the radial direction forming transmembrane pressure, which is the driving force for the filtration process. When water goes through the membrane into permeate flow, it always presents a pressure drop region in the membrane called transmembrane pressure. It's the motivation of filtration to ensure water flows through the membrane. Besides, from the 180s to the 3500s, the pressure on the inlet and outlet are stable. The highest pressure is 236 kPa at 3500s, and the lowest is 11 kPa at the permeate outlet. This behavior shows that the filtration process is highly efficient while maintaining a stable pressure in the module and membrane for a long time.

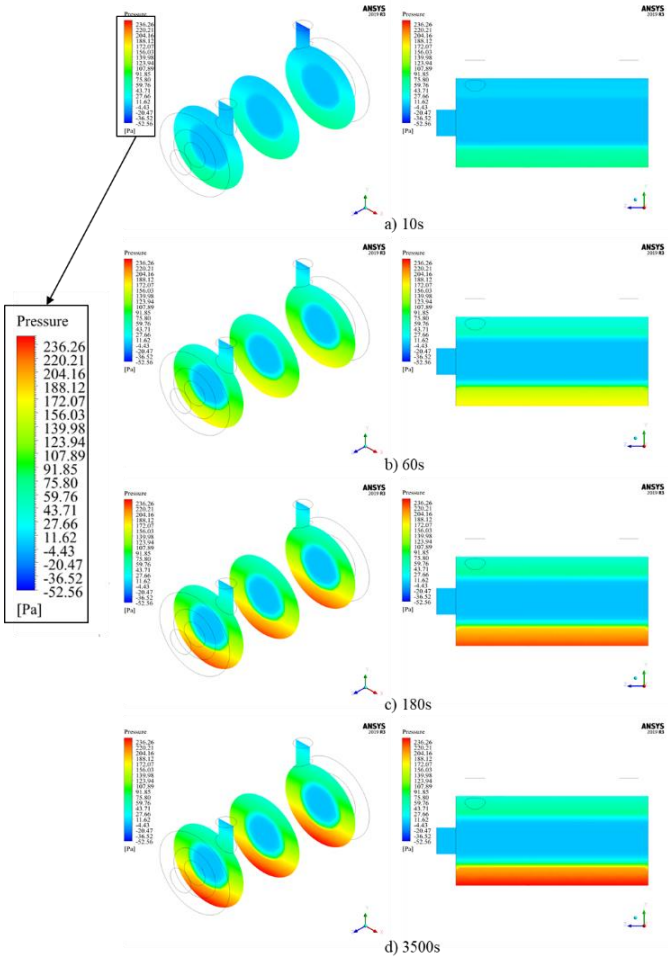

Figure 9 Distribution of pressure in the module

3.6 Performance Of Membrane Module And Validation

Based on the results of Table 3 for the mass flow of water and bromelain at the inlet and outlet, 99% of bromelain exits the equipment at the concentrate outlet in comparison to the input source, and the bromelain composition at the concentrate outlet is 37.73 %, higher than input 4.4%, 18.3% of water flow has been filtered. The low bromelain mass flow at the permeate outlet indicates that the filtration is efficient when almost the protein does not pass through the membrane, and most of the bromelain is collected at the outlet concentrate. Bromelain loss at the concentrate outlet is caused by a small part adhering to the membrane surface, which hinders the filtration process. The bromelain was isolated and purified to confirm the simulation results, as described in section 4. The results demonstrated that the actual values obtained from the experiment gave the bromelain's mass concentrated outlet of 4.88 g/s and the water's mass concentrated outlet of 8.03 kg/s. It was close to the simulation values. Additionally, the coefficient of variation of the model is nearly accurate (<10%). Therefore, this model can be used to simulate and control the purification process of bromelain.

Table 3 Mass Flow Of Bromelain And Water

Parameters	Simulation results		Experimental results	
	Water	Bromelain	Water	Bromelain
Inlet (g/s)	10	5	10	5
Permeate outlet (g/s)	1.82	$1.199.10^{-4}$	1.67	$1.094.10^{-4}$
Concentrated outlet (g/s)	8.17	4.95	8.03	4.88

4.0 CONCLUSION

In this study, the proposed mathematical model effectively predicts the fluid dynamics of enzyme bromelain inside the UF; The volume fraction of water decreases with time until the water no longer passes through the membrane. The volume fraction of bromelain increased with time, and bromelain was concentrated mainly and below the machine, reaching a maximum value of 0.608. The volume ratio of bromelain at the concentrate outlet has a maximum value of 0.37. Over time the amount of bromelain concentrates around the membrane surface as much as possible, causing membrane clogging, concentration polarization, and hindering the filtration process. About 99.17% of bromelain is recovered at the outlet of the concentrate, and small bromelain contents remain on the membrane surface or exit at the permeation stream. In addition, the results demonstrate that the actual values obtained from the experiment for the mass of bromelain concentrate are 0.00488 kg/s, and the coefficient of variation of the model is almost accurate (<10%). Therefore, this model can simulate and control the bromelain purification process.

Acknowledgement

We acknowledge Ho Chi Minh City University of Technology (HCMUT), VNU-HCM for supporting this study.

References

[1] Ali, M.M., Hashim, N., Abd Aziz, S., Lasekan, O., 2020. Pineapple (Ananas comosus): A comprehensive review of nutritional values, volatile compounds, health benefits, and potential food products. *Food Research International* 137: 109675.

[2] Samreen, C.V. V., Edukondalu, L., Beera, V., Rao, V.S., 2020. Physicochemical characteristics of pomegranate and pineapple juice. *Indian Journal of Ecology* 43: 60–3.

[3] Kasa, T., Yohanis, F.G., 2017. Chemical composition and nutritional effect of pineapple, mango, banana, avocado and orange: A review article. Chemical and Process Engineering

Research 54: 1–6.
[4] Hossain, M.F., Akhtar, S., Anwar, M., 2015. Nutritional value and medicinal benefits of pineapple. International Journal of Nutrition and Food Sciences 4(1): 84–8.
[5] Nor, M.Z.M., Ramchandran, L., Duke, M., Vasiljevic, T., 2015. Characteristic properties of crude pineapple waste extract for bromelain purification by membrane processing. *Journal of Food Science and Technology* 52(11): 7103–12.
[6] Banerjee, S., Ranganathan, V., Patti, A., Arora, A., 2018. Valorisation of pineapple wastes for food and therapeutic applications. *Trends in Food Science & Technology* 82: 60–70.
[7] Kumar, R., Kumar, R., Sharma, N., Khurana, N., Singh, S.K., Satija, S., et al., 2022. Pharmacological evaluation of bromelain in mouse model of Alzheimer's disease. *NeuroToxicology* 90: 19–34.
[8] Hale, L.P., Greer, P.K., Trinh, C.T., James, C.L., 2005. Proteinase activity and stability of natural bromelain preparations. *International Immunopharmacology* 5(4): 783–93.
[9] Devakate, R. V., Patil, V. V., Waje, S.S., Thorat, B.N., 2009. Purification and drying of bromelain. *Separation and Purification Technology* 64(3): 259–64.
[10] Mohan, R., Sivakumar, V., Rangasamy, T., Muralidharan, C., 2016. Optimisation of bromelain enzyme extraction from pineapple (Ananas comosus) and application in process industry. *American Journal of Biochemistry and Biotechnology* 12(3): 188–95.
[11] Baidhe, E., Kigozi, J., Mukisa, I., Muyanja, C., Namubiru, L., Kitarikawe, B., 2021. Unearthing the potential of solid waste generated along the pineapple drying process line in Uganda: A review. *Environmental Challenges* 2: 100012.
[12] Girard, B., Fukumoto, L.R., 2000. Membrane processing of fruit juices and beverages: a review. *Critical Reviews in Food Science Nutrition* 40(2): 91–157.
[13] Hinkova, A., Bubnık, Z., Kadlec, P., Pridal, J., 2002. Potentials of separation membranes in the sugar industry. *Separation and Purification Technology* 26(1): 101–10.
[14] Lipnizki, F., 2010. Membrane processes for the production of bulk fermentation products. *Membrane Technology,* 121–53. Elsevier
[15] Bilici, Z., Keskinler, B., Dizge, N., 2020. Protein and lactose separation by modified ultrafiltration membrane using layer by layer technique. *Journal of Membrane Science and Research* 6(2): 211–7.
[16] Lopes, F.L.G., Severo Júnior, J.B., Souza, R.R. de., Ehrhardt, D.D., Santana, J.C.C., Tambourgi, E.B., 2009. Concentration by membrane separation processes of a medicinal product obtained from pineapple pulp. *Brazilian Archives of Biology and Technology* 52: 457–64.
[17] Nor, M.Z.M., Ramchandran, L., Duke, M., Vasiljevic, T., 2016. Separation of bromelain from crude pineapple waste mixture by a two-stage ceramic ultrafiltration process. *Food and Bioproducts Processing* 98: 142–50.
[18] Doko, M.B., Bassani, V., Casadebaig, J., Cavailles, L., Jacob, M., 1991. Preparation of proteolytic enzyme extracts from Ananas comosus L., Merr. fruit juice using semipermeable membrane, ammonium sulfate extraction, centrifugation and freeze-drying processes. *International Journal of Pharmaceutics* 76(3): 199–206.
[19] Haribabu, M., Dunstan, D.E., Martin, G.J.O., Davidson, M.R., Harvie, D.J.E., 2020. Simulating the ultrafiltration of whey proteins isolate using a mixture model. *Journal of Membrane Science* 613(May): 118388, Doi: 10.1016/j.memsci.2020.118388.
[20] Marcos, B., Moresoli, C., Skorepova, J., Vaughan, B., 2009. CFD modeling of a transient hollow fiber ultrafiltration system for protein concentration. *Journal of Membrane Science* 337(1–2): 136–44, Doi: 10.1016/j.memsci.2009.03.036.
[21] Angeli, S.D., Pilitsis, F.G., Lemonidou, A.A., 2015. Methane steam reforming at low temperature: Effect of light alkanes' presence on coke formation. *Catalysis Today* 242: 119–28.
[22] Duong, Y.H.P., Vo, N.T., Le, P.T.K., Tran, V.T., 2021. Three-Dimensional Simulation of Solar Greenhouse Dryer. *Chemical Engineering Transactions* 83: 211–6.
[23] Abreu, D.C.A., Figueiredo, K.C. de S., 2019. Bromelain Separation and Purification. *Brazilian Journal of Chemical Engineering* 36(02): 1029–39.
[24] Oliveira Neto, G.L., Oliveira, N.G.N., Delgado, J.M.P.Q., Nascimento, L.P.C., Magalhães, H.L.F., Oliveira, P.L. de., et al., 2021. Hydrodynamic and performance evaluation of a porous ceramic membrane module used on the water–oil separation process: An investigation by CFD. Membranes 11(2): 121.
[25] Manual, U.D.F., 2009. *Ansys Fluent* 12.0. Theory Guide.
[26] Kleinstreuer, C., Griffith, P., 2004. Two-Phase Flow: Theory and Applications. *Applied Mechanics Reviews* 57(4): B22.
[27] Schiller, L., 1933. A drag coefficient correlation. Zeitschrift des Vereins Deutscher Ingenieure 77: 318–320.
[28] Petkov, P., Tsiulyanu, D., Kulisch, W., Popov, C., 2015. Nanoscience advances in CBRN agents detection, information and energy security. Springer.
[29] Chen, H., Tang, J., Liu, F., 2006. Coupled simulation of an electromagnetic heating process using the finite difference time domain method. *Journal of Microwave Power and Electromagnetic Energy* 41(3): 50–68.
[30] Josijević, M.M., Šušteršič, V.M., Gordić, D.R., 2020. Ranking energy performance opportunities obtained with energy audit in dairies. *Thermal Science* 24(5 Part A): 2865–78.
[31] Khairunnisa, F.A., Vedder, M., Evers, L., Permana, S., 2018. Bromelain content of extract from stem of pineapple (Ananas comosus (L.) Merr). *AIP Conference Proceedings,* 2019. AIP Publishing LLC p. 20014.
[32] Campos, D.A., Coscueta, E.R., Valetti, N.W., Pastrana-Castro, L.M., Teixeira, J.A., Picó, G.A., et al., 2019. Optimization of bromelain isolation from pineapple byproducts by polysaccharide complex formation. *Food Hydrocolloids* 87: 792–804.